International Journal of Medical Microbiology 314 (2024) 151603

Contents lists available at ScienceDirect

International Journal of Medical Microbiology

journal homepage: www.elsevier.com/locate/ijmm

Impact of *Mycobacteroides abscessus* colony morphology on biofilm formation and antimicrobial resistance

Anna Maria Oschmann-Kadenbach [a,b], Christoph Schaudinn [c], Leonard Borst [b], Carsten Schwarz [d], Katharina Konrat [a], Mardjan Arvand [a], Astrid Lewin [b,*]

[a] Unit 14 Hospital Hygiene, Infection Prevention and Control, Robert Koch Institute, Seestr. 10, Berlin, Germany
[b] Unit 16 Mycotic and Parasitic Agents and Mycobacteria, Robert Koch Institute, Seestr. 10, Berlin, Germany
[c] Unit ZBS4 Advanced Light and Electron Microscopy, Robert Koch Institute, Seestr. 10, Berlin, Germany
[d] CF Center Westbrandenburg, Division Cystic Fibrosis, Health and Medical University Potsdam and Clinic Westbrandenburg, Hebbelstraße 1, 14467 Potsdam, Germany

ARTICLE INFO

Keywords:
Nontuberculous mycobacteria
Mycobacteroides abscessus
Biofilm
Antibiotic resistance
Disinfectant tolerance
Colony morphotype

ABSTRACT

Mycobacteroides abscessus is one of the most resistant bacteria so far known and causes severe and hard to treat lung infections in predisposed patients such as those with Cystic Fibrosis (CF). Further, it causes nosocomial infections by forming biofilms on medical devices or water reservoirs. An eye-catching feature of *M. abscessus* is the growth in two colony morphotypes. Depending on the presence or absence of glycopeptidolipids on the cell surface, it forms smooth or rough colonies. In this study, a porous glass bead biofilm model was used to compare biofilm formation, biofilm organization and biofilm matrix composition in addition to the antimicrobial susceptibility of *M. abscessus* biofilms versus suspensions of isogenic (smooth and rough) patient isolates. Both morphotypes reached the same cell densities in biofilms. The biofilm architecture, however, was dramatically different with evenly distributed oligo-layered biofilms in smooth isolates, compared to tightly packed, voluminous biofilm clusters in rough morphotypes. Biofilms of both morphotypes contained more total biomass of the matrix components protein, lipid plus DNA than was seen in corresponding suspensions. The biofilm mode of growth of *M. abscessus* substantially increased resistance to the antibiotics amikacin and tigecycline. Tolerance to the disinfectant peracetic acid of both morphotypes was increased when grown as biofilm, while tolerance to glutaraldehyde was significantly increased in biofilm of smooth isolates only. Overall, smooth colony morphotypes had more pronounced antimicrobial resistance benefit when growing as biofilm than *M. abscessus* showing rough colony morphotypes.

1. Introduction

Mycobacteroides (*M.*) *abscessus*, also called *Mycobacterium abscessus,* is an opportunistic pathogen belonging to the group of nontuberculous mycobacteria (NTM). *M. abscessus* exhibits an extreme tolerance towards antimicrobials and belongs to the most resistant mycobacterial species (Petrini, 2006). It appears in patients with underlying respiratory disease such as cystic fibrosis (CF) or non-CF bronchiectasis. As treatment of *M. abscessus* infections often includes a prolonged combination of up to five antibiotics over months or even years, and may lead to severe side effects, comprehensive susceptibility testing is essential to evaluate the best treatment options (Benwill and Wallace, 2014).

Besides its outstanding resistance towards antibiotics, the tolerance of *M. abscessus* to disinfectants has also come to the fore (Primm et al., 2004). In the past decades, an arising amount of nosocomial infections caused by NTM has been reported (Phillips and von Reyn, 2001). The route of infection can often be traced back to biofilm-colonized medical devices, such as heater-cooler units. The most influential outbreak of NTM in past years has been the contamination of HCUs by *M. chimaera* (Riccardi et al., 2020). Meanwhile, other NTM species, including

Abbreviations: AMI, amikacin; CF, Cystic Fibrosis; CFU, colony forming units; CLSI, Clinical & Laboratory Standards Institute; eDNA, extracellular DNA; GA, glutaraldehyde; geq, genome equivalents; GPL, glycopeptidolipid; *gpl*, glycopeptidolipid gene cluster; *M. abscessus*, *Mycobacteroides abscessus*; MB, Middlebrook medium; NTM, Nontuberculous mycobacteria; PGB, porous glass beads; PMA, Propidium monoazide; PAA, peracetic acid; TGC, tigecycline; TLC, thin layer chromatography.

* Correspondence to: Unit 16 Mycotic and Parasitic Agents and Mycobacteria, Robert Koch Institute, Seestr. 10, 13353 Berlin, Germany.
E-mail address: LewinA@rki.de (A. Lewin).

https://doi.org/10.1016/j.ijmm.2024.151603
Received 5 October 2023; Received in revised form 15 January 2024; Accepted 15 January 2024
Available online 18 January 2024

M. abscessus, have also been found growing in such devices (Baker et al., 2017), where they form biofilms protecting them against the common disinfection procedures (Falkinham, 2020) (Schreiber et al., 2016). Also, *M. abscessus* has been reported to form biofilms in the lung cavities of affected patients (Qvist et al., 2015), which is assumed to further promote their antibiotic resistance (López-Roa et al., 2022). All things considered, there is an urgent need to explore the mechanism and consequences of biofilm formation of *M. abscessus*.

The ability of *M. abscessus* to form biofilms has been linked to its colony morphology (Clary et al., 2018). The colony morphology of *M. abscessus*, in turn, is based on the presence or absence of glycopeptidolipids (GPL) on the cell surface. Several studies have shown that rough morphotypes with mutations in the GLP synthesis and transport genes accumulate in patients during chronic infection (Kreutzfeldt et al., 2013; Lewin et al., 2021; Pawlik et al., 2013). The presence of rough isolates enhanced the virulence in cell or murine models, which was linked to their ability to replicate in macrophages and escape phagosomes (Bernut et al., 2014; Kim et al., 2019). Furthermore, it was shown that rough *M. abscessus* variants induced more IFNβ- and TNFα in mouse macrophages than smooth variants (Ruangkiattikul et al., 2019). Rough *M. abscessus* variants have been thought to not form biofilms at all (Howard et al., 2006). Although this assumption has been disproved (Clary et al., 2018), until now, surface-attached biofilms of smooth and rough *M. abscessus* variants were not compared with respect to their architectural features and antimicrobial resistance.

Even though the formation of biofilms in patients infected by *M. abscessus* is known, susceptibility testing still relies on the use of suspended bacteria following the CLSI recommendations (Woods and Conville, 2011). These suspensions often display higher susceptibility than biofilm-associated bacteria and it has been reported that the outcome of the susceptibility testing for patient isolates often does not correlate with treatment success (van Ingen and Kuijper, 2014).

Considering the interplay of colony morphology, biofilm formation and antimicrobial resistance, the aim of the present study was to compare the ability of rough and smooth *M. abscessus* morphotypes to form biofilms in a biofilm bead model, analyze the architecture and composition of these biofilms, and evaluate the effect of biofilm formation in rough and smooth isolates on their resistance to antibiotics and tolerance toward disinfectants.

2. Materials and methods

2.1. M. abscessus isolates

The four *M. abscessus* subsp. *abscessus* isolates 25/14^{sm}, 35/14^{rg}, 09/13^{sm}, and 58/15^{rg} used in this study (Table 1) were obtained from respiratory samples from two patients (patients 1 and 2) with CF. A rough and a smooth derivative from the same strain (Suppl. Fig. 1 A) isolated from each patient underwent whole genome sequencing (Lewin et al., 2021), which allowed comparison of the *gpl* gene clusters using Geneious Prime ® (2020.2.3, Biomatters, Ltd., New Zealand).

The GPL of all isolates were isolated and analyzed by thin layer chromatography (Suppl. Fig. 1 C) as described before (Kirubakar et al., 2020).

Table 1
M. abscessus subsp. *abscessus* isolates used in the study.

Isolate name	Patient	Morphotype
25/14^{sm}	1	Smooth
35/14^{rg}	1	Rough
09/13^{sm}	2	Smooth
58/15^{rg}	2	Rough

2.2. Cultivation of biofilm

Biofilms were cultivated on beads based on the protocol of a biofilm bead assay established for *Pseudomonas aeruginosa* (Konrat et al., 2016; Zoppo et al., 2020). Depending on the analysis, different bead types were tested, including glass beads (GB; Merck KGaA, Germany), polytetrafluoroethylene (PTFE) beads (PB; Hoch Kugelfertigung, Germany), porous glass beads (PGB; ROBU® Glasfilter-Geraete GmbH, Germany) and glass beads coated with collagen [CGB; collagen was prepared according to manufacturer's instructions (Merck KgaA, Germany) and each GB was covered with 30 µl collagen and dried at room temperature]. After evaluating the biofilm formation by using these bead types, the cultivation of biofilm was continued with PGBs, because these beads exhibited the highest number of bacteria in their biofilms. These beads have the shape of a cylinder with a flat, 4 mm surface at the bottom and a hemisphere-shaped tip (Suppl. Fig. 2 A-C). Sterile beads were placed in a 24-well plate and incubated with 1 ml of Middlebrook 7H9 broth + 10% OADC [MB-OADC broth (Becton Dickinson GmbH)] containing 10^5 colony forming units (CFU) of *M. abscessus*. The inoculated beads were incubated at 37 °C on an orbital shaker with 8 mm amplitude at 150 rpm for as long as further analysis required. Afterwards, the CFU was determined. To this aim, each bead was washed by dipping twice in sterile water and transferring it to a tube containing 1 ml of sterile water. The beads were then sonicated for 20 min at 40 kHz using the BactoSonic®, (Bandelin), which is constructed specifically to detach biofilm and individualize the bacteria without compromising the bacteria. The individualized bacteria were plated by 5 µl spot-plating on Middlebrook Seven H11 + 10% OADC plates (MB-OADC agar) (Becton Dickinson GmbH). The plates were incubated for five to seven days at 37 °C and the number of bacteria determined by CFU counting

To examine the efficacy of the sonication, biofilm of *M. abscessus* 25/14^{sm} was cultivated as described above. Three beads with and without sonication, respectively, were stained with SYTO™9 (Thermo Fisher Scientific Inc) and PI (propidium iodide, Thermo Fisher Scientific Inc). For staining, a mixture of 1:1 H_2O/DMSO was prepared and the stains added to a concentration of 1:1000. A total of 50 µl of the staining solution was added to the biofilm beads and incubated for 30 min in the dark. Afterwards the beads were carefully washed by dipping in fresh water and placed on a glass slide and imaged by confocal laser scanning microscopy (LSM780, Carl Zeiss AG). Settings were adjusted for optimal brightness and contrast.

2.3. Quantification of M. abscessus in biofilm

Accumulation of bacteria in biofilms on PGBs was quantified by incubating the biofilms for different periods of time (1, 2, 3, 7 and 10 days) and determining the CFU/bead as described above. Additionally, the metabolic activity was analyzed by measuring the ATP amount by using the BacTiter-Glo™ Microbial Cell Viability Assay (Promega GmbH) following the manufacturers protocol.

Quantification of living bacteria in the biofilms was performed by counting of CFU and by determination of genome equivalents (geq) by qPCR with PMA (propidium monoazide; 20 mM in H_2O, Biotium). Confirmation that PMA-qPCR works for both, smooth and rough isolates, had been obtained by pre-tests (data not shown). For geq quantification, 100 µl of the sonicated biofilm sample were transferred to a fresh tube. PMA was added following the manufacturer's recommendations. After incubation at room temperature for 10 min, the samples were exposed for 5 min to blue light (~ 470 nm) to activate the PMA. Afterwards, the samples were centrifuged at 12,000 g for 10 min at 4 °C and the supernatants discarded to avoid further binding of PMA to the DNA. The pellets were resuspended in 100 µl of sterile water and the mixture was heated for 30 min at 96 °C in order to make the DNA available for TaqMan-qPCR. The primers Mabs rpoB-FW (CGATAGAGGACTTCGCCTAACC) and Mabs rpoB-BW (TCGAGCACGTAAACTCCCTTTC) and the probe Mabs rpoB-Probe ([FAM]-

CCACTGACCGAACATCTATCCCGC-[TAMRA]) (Steindor et al., 2015) were used to amplify a part of the *rpoB* gene. The qPCR was performed using the DreamTaq Polymerase (Thermo Fisher Scientific Inc.) and an Agilent AriaMx Real-time PCR system (Agilent) with the following thermal profile: 10 min 95 °C, followed by 40 cycles of 30 s 95 °C, 30 s 60 °C, 1 min 72 °C, and one final step for 6 min at 72 °C. The amount of DNA per sample was calculated using a DNA standard and the geq of each sample were calculated on the basis of the genome weight of each isolate.

2.4. Determination of the biofilm structure by scanning electron microscopy

Biofilms were cultivated as described above for 7 days and fixed with 4% paraformaldehyde/10% glutaraldehyde for 24 h at 4 °C.

After fixation, the samples were dehydrated in a graded ethanol line (30, 50, 70, 90, 95, 100%) and dried overnight in hexamethyldisilazane. Then, the beads were mounted on aluminum stubs and sputter coated with 16 nm gold-palladium, and imaged in the SEM (ZEISS 1530 Gemini, Carl Zeiss Microscopy GmbH) operating at 3 kV using the in-lens electron detector.

The images were processed for optimal brightness and contrast using Affinity Photo (©Serif (Europe) Ltd., Version 2.0 Nov'22). All modifications were applied to the whole image.

2.5. Quantification of amounts of DNA, proteins and lipids in biofilms and suspension cultures

For quantification of DNA, proteins and lipids in biofilm, 24 beads with *M. abscessus* biofilm cultivated for 7 days were collected in a falcon tube containing 30 ml of sterile water; for suspension, five agar plates that had been incubated for 7 days (MB-OADC) were washed away with 6 ml of water each, and the resuspended bacteria suspensions were collected in a falcon tube. Then, the samples were sonicated and the supernatants of the biofilm samples were transferred to a fresh falcon tube in order to remove the PGBs. The number of viable bacteria present in each sample was determined by PMA-qPCR as described above.

Quantification of DNA: For quantification of DNA, 100 µl of each bulk sample were transferred to fresh tubes and qPCR was performed as described above. After qPCR the DNA/ml of each sample was determined by using a DNA standard. Finally, the amount of DNA per bacterium was calculated.

Quantification of protein: A protein standard of mycobacterial proteins was produced as described before (Lewin et al., 2003). The protein concentration was determined with the Pierce™ BCA protein Assay (Thermo Fisher Scientific Inc) by following the manufacturer's protocol. 50 µl of each sample and of dilutions of the mycobacterial protein standard were transferred to the wells of a Greiner black-well plate with transparent bottom (Greiner Bio-One International GmbH). Afterwards, 50 µl of a staining solution composed of 0.2% SYPRO™ Orange protein gel stain (Thermo Fisher Scientific Inc.) in DMSO was added to each well and carefully mixed by pipetting. The plate was sealed and incubated in the dark for 30 min at room temperature. Then, the fluorescence was measured at $470_{Ex}/570_{Em}$ using a TECAN microplate reader (TECAN Trading AG). A standard curve was calculated and for each sample the amount of protein/ml determined. Finally, the amount of protein per bacterium was calculated for each sample.

Quantification of lipid: 10 ml of each bulk sample were transferred to fresh falcon tubes and centrifuged at 8000 g for 10 min at 4 °C. The supernatant was discarded and the pellet resuspended in a mixture of 2:1 chloroform/methanol. The samples were incubated overnight at room temperature. Afterwards, the samples were centrifuged again and the supernatant transferred to a pre-weighed falcon tube. The liquid was evaporated completely. Finally, the tubes containing the isolated lipids were weighed again and the amount of lipids per ml determined. Further, the amount of lipid per bacterium was calculated.

2.6. Susceptibility determination of bacteria in biofilm and suspension to the antibiotics amikacin and tigecycline

The susceptibility of biofilm and bacteria in suspension was tested by micro-dilution with different concentrations of amikacin (AMI) (0 – 128 µg/ml) and tigecycline (TGC) (0 – 8 µg/ml).

The biofilm samples were cultivated as described above for 7 days. The suspension was produced following the CLSI recommendation M24-A2, update M62, for susceptibility testing using a micro dilution method with adjustments, such as counting cfu instead of visually assessing growth by turbidity observation and reporting of MIC. Briefly, the bacteria were grown on MB-OADC for 7 days. Afterwards, one colony was taken off the plate and resuspended in Mueller-Hinton II broth (cation-adjusted; Becton Dickinson GmbH) and diluted to a CFU of 10^8/ml. Biofilm beads or 1 ml of the suspension, respectively, were transferred into the wells of 48-well plates with different concentrations of the corresponding antibiotic. The test plates were sealed with a lid and further incubated at 30 °C for 5 days without shaking. Afterwards, the CFU was determined as described above.

2.7. Tolerance determination of bacteria in biofilm and suspension to the disinfectants glutaraldehyde and peracetic acid

Peracetic acid (PAA) (Wofasteril 40%, Kesla Pharma Wolfen GmbH) was tested at concentrations of 0.01%, 0.05%, 0.075%, 0.1%, and 0.5% (v/v); glutaraldehyde (GA) (25%, Merck KGaA) was used at concentrations of 0.1%, 0.5%, 1%, 2%, and 5% (v/v). Prior to the testing, the neutralization of the highest concentration of disinfectant and the toxicity of the neutralization buffer itself were evaluated as described before (Konrat et al., 2016). For the neutralization of PAA, 0.5% sodium sulfite in phosphate buffer (0.1 M, pH 7.8) was used, and for neutralization of GA, 1% glycine + 0.05% Tween 80 in phosphate buffer (0.1 M, pH 7.8), was employed. The disinfectant stock solutions were titrated.

The procedure to determine tolerance towards PAA and GA was described by Konrat et al. (Konrat et al., 2016). For testing suspension, bacteria grown on MB-OADC agar for 7 days were washed off the whole plate with 0.1% Tween 80. The resuspended bacteria were washed 3x by centrifugation (3000 rpm, 4 °C, 10 min) and resuspension in 0.1% Tween 80. Then, the suspension was diluted in 0.1% Tween 80 to a CFU of 10^8/ml. The disinfectant testing was following the EN 14348. Therefore, per concentration three tubes containing 900 µl of a 1:10 concentration of the disinfectant was prepared and tempered for 10 min to 20 °C. Afterwards, 100 µl bacterial suspension was added and incubated for 60 min at 20 °C. Thereafter the tubes were vortexed and 100 µl of the mixture transferred to a fresh tube containing 900 µl neutralizer (4 °C).

The biofilm beads were also cultivated for 7 days as described before. Briefly, for each concentration three tubes containing 200 µl of disinfectant were prepared and tempered to 20 °C for 10 min. Thereafter one bead per tube was taken from the cultivation plate using sterile tweezers, carefully washed by dipping twice in sterile water and directly put into the disinfectant. The beads were incubated for 60 min after which 1.8 ml of neutralizer were added to the tube and mixed well by pipetting.

After neutralization, biofilm and suspension samples were placed in a sonicator to detach and individualize the bacteria as described above for 20 min. Then, the samples were diluted in steps of 10 in the according neutralizer and plated by drop-plating on MB-OADC 10% agar plates. The plates were incubated for 7 days at 37 °C after which the CFU was counted.

All experiments were performed at least three times, with three technical replicates per experiment.

Successful disinfection was defined in accordance with EN 14348 as achieving at least 4 $\log_{10}$ reduction in mean viable CFU.

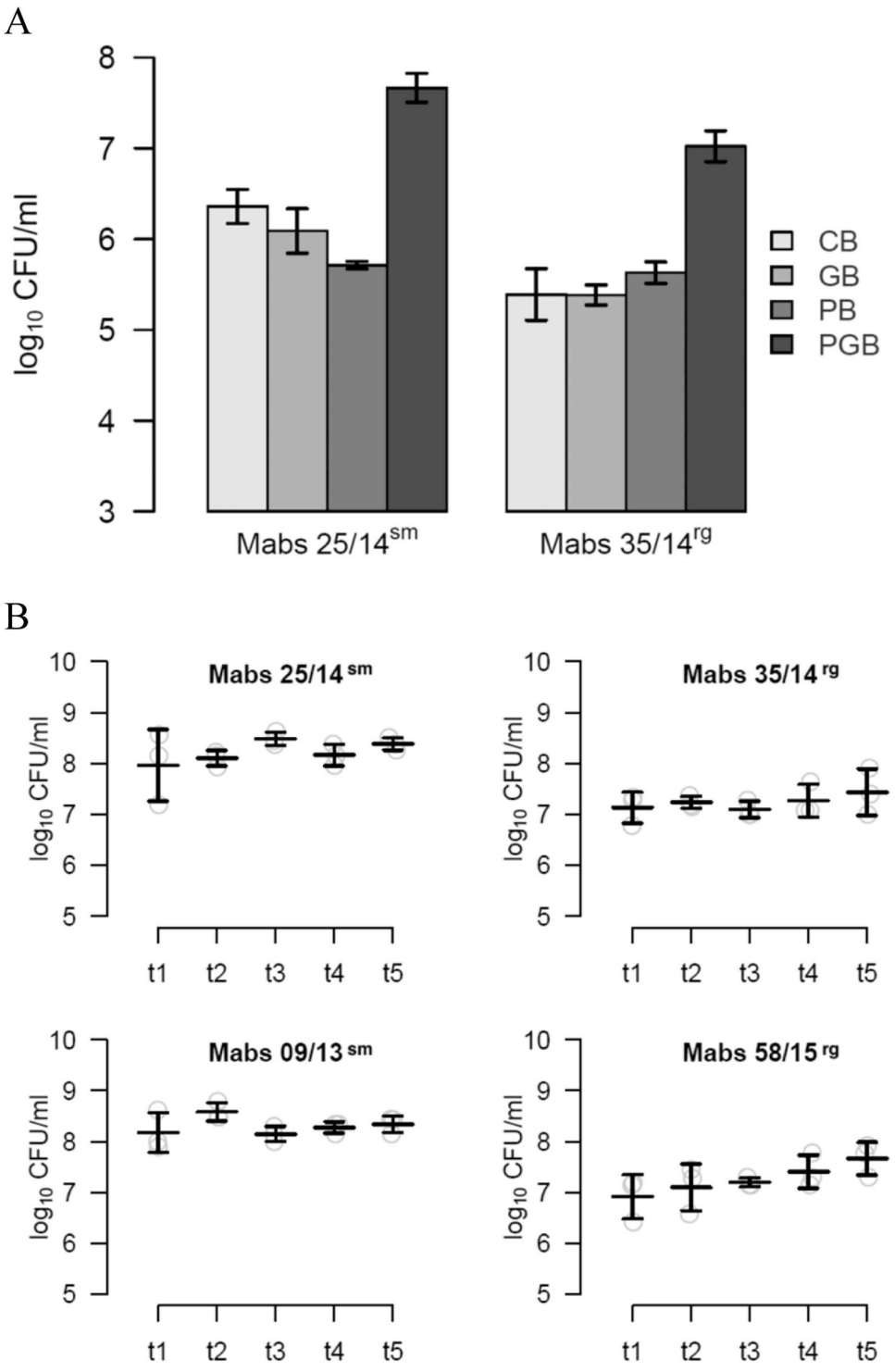

Fig. 1. Biofilm formation on different types of beads and reproducibility of biofilm growth. A) *M. abscessus* isolates 25/14^{sm} and 35/14^{rg} were grown for 7 days in MB-OADC as biofilm on different bead types. Bacteria were removed from beads and suspended in 1 ml of water. Both isolates grew best on PGBs. The smooth isolate *M. abscessus* 25/14^{sm} reached a $\log_{10}$ CFU/bead of approx. 7.8 and the rough counterpart *M. abscessus* 35/14^{rg} reached a $\log_{10}$ CFU/bead of approx. 7. On the other beads the smooth isolate reached a maximum of 6.5 $\log_{10}$ CFU/bead on CBs while the rough isolate reached a maximum of 5.8 $\log_{10}$ on PBs. B) Reproducibility of biofilm growth. For each isolate, biofilms on five individual biological replicates (t1-t5) were grown for 7 days and quantified. Displayed are mean and standard deviation of technical triplicates. CB: collagen coated beads; GB: glass beads; Mabs: *M. abscessus*; MB-OADC: Middlebrook 7H9 broth + 10% OADC; PB: PTFE beads; PGB: porous glass beads.

3. Results

3.1. Genetic and phenotypic characterization of M. abscessus isolates

The Suppl. Fig. 1 summarizes the characterization of the isolates 09/13^{sm}, 58/15^{rg}, 25/14^{sm}, 35/14^{rg} that were used in this study. Suppl. Fig. 1 A shows the rough (35/14^{rg} and 58/15^{rg}) and smooth (25/14^{sm} and 09/13^{sm}) colony morphotypes.

Genetic analysis (Suppl. Fig. 1 B) showed that the *mps2* genes in the isolates 25/14^{sm} and 35/14^{rg} [both obtained from patient 1] differed by a deletion of the nucleotides A and T in isolate 35/14^{rg} at the positions 5191 and 5192. This results in a frameshift explaining the morphological change from smooth to rough. In the second pair, 09/13^{sm} and 58/15^{rg} (both obtained from patient 2), the frameshift in isolate 58/15^{rg} resulted from the insertion of the nucleotide C at the position 5189 of the *mps2* gene, also explaining the morphological transformation (Suppl. Fig. 1 B). Isolates 09/13^{sm} and 58/15^{rg} differed in addition to the *mps2* gene in the gene MAB_1881c. By whole genome sequencing of all four isolates (Lewin et al., 2021) it could be excluded that the patients were infected by different *M. abscessus* strains proving that 09/13^{sm} and

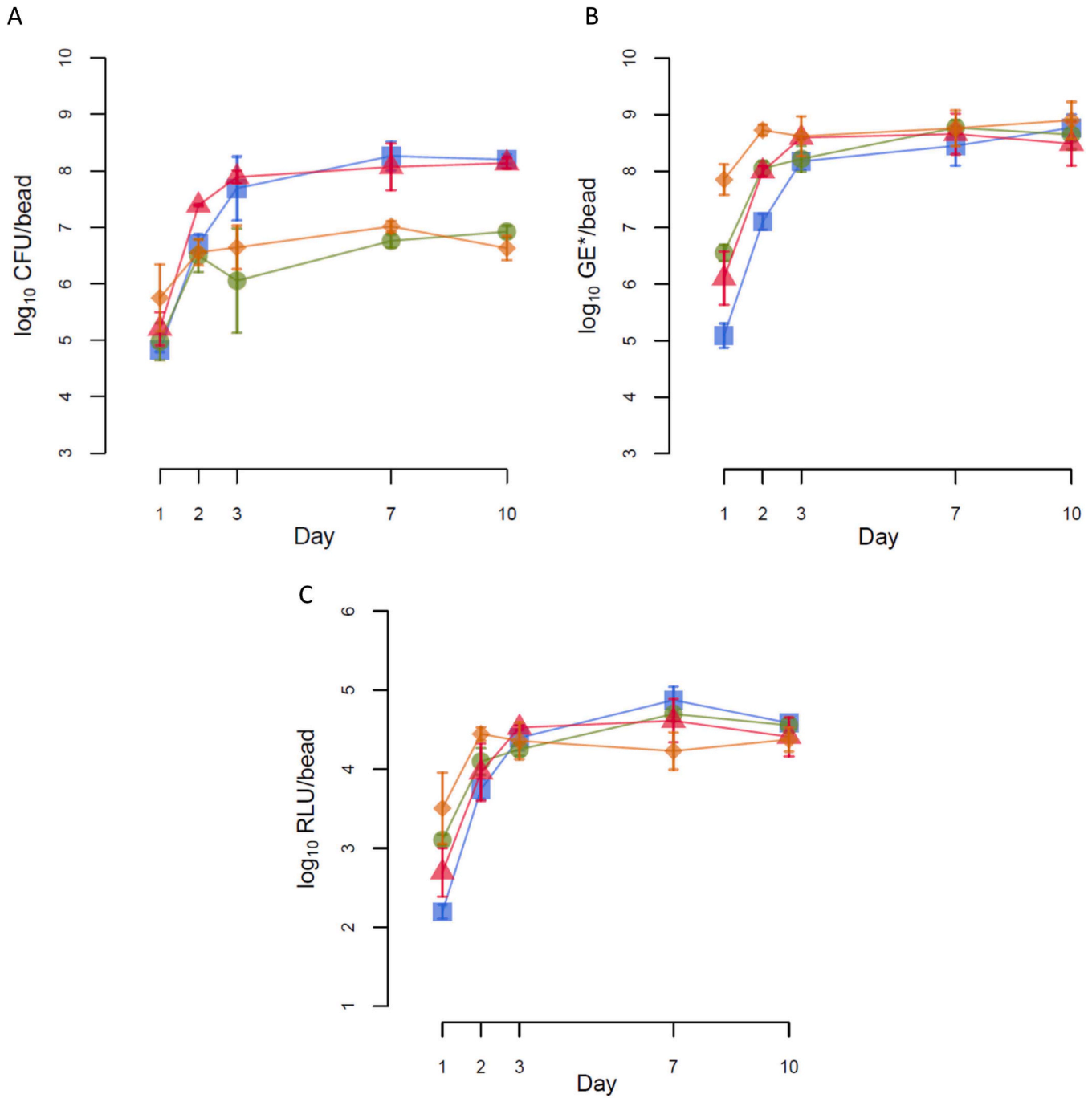

Fig. 2. Quantification of *M. abscessus* isolates in biofilm. The *M. abscessus* isolates were cultivated for 10 days in MB-OADC on PGBs and quantified by CFU, qPCR with PMA and ATP measurement. All four strains reached a stationary phase after 5 days of cultivation. While in CFU/bead (A) the smooth and rough isolates displayed a difference of approx. 1 $\log_{10}$ CFU from day 3 on, this difference was not visible in the qPCR with PMA (B) or the ATP measurement (C). The values show means and standard deviations of three biological replicates. Blue line: Mabs 25/14^{sm}, Green line: Mabs 35/14^{rg}, Red line: Mabs 09/13^{sm}, Orange line: Mabs 58/15^{rg}. MB-OADC: Middlebrook 7H9 broth + 10% OADC; Mabs: *M. abscessus*; PGB: porous glass beads; PMA: Propidium monoazide.

58/15^{rg} as well as 25/14^{sm} and 35/14^{rg} are derivatives from the same strains, respectively.

Confirmation that the smooth/rough morphotypes were caused by presence/lack of GPL was obtained by TLC (Suppl. Fig. 1 C), which showed that both smooth isolates produced GPL with an identical pattern, while the rough isolates contained no visible GPL (Suppl. Fig. 1 C).

3.2. Biofilm formation on PGBs

In order to identify the most suitable bead type for the cultivation of biofilms of smooth and rough *M. abscessus*, four different types of beads exhibiting different surface structures were tested. The surface materials were either glass, PTFE or collagen and additionally two types of glass beads with either even/smooth or coarse/rough surface structure were tested.

The highest numbers of bacteria were achieved, when the biofilms were cultivated on porous glass beads. While the biofilms grown on PGBs contained almost 8 $\log_{10}$ CFU/bead for *M. abscessus* 25/14^{sm} and around 7 $\log_{10}$ CFU/bead for *M. abscessus* 35/14^{rg}, the biofilms grown on the other bead types showed 1 – 1.5 $\log_{10}$ less bacteria per bead (Fig. 1 A).

To confirm that the number of mycobacteria per biofilm was stable and reproducible among multiple trials, the CFU/bead of five biological samples per strain were analyzed. Each isolate produced similar bacterial loads in the five individual replicates after 7 days (max. +/- 0.5 $\log_{10}$), while the means between smooth and rough isolates differed by 1.0 – 1.5 $\log_{10}$ (Fig. 1 B).

Confirmation that the biofilm was fully detached from the porous glass beads by sonication was achieved by microscopic analysis showing that after sonication no residual biofilm was found on the PGBs (Suppl. Fig. 2 D).

The number of bacteria in the biofilm on a given PGB was measured by means of geq by qPCR with PMA, by ATP quantification and by CFU determination (Fig. 2). The amount of genome equivalents and the metabolic activity (ATP amount) of all four isolates were very similar showing no difference between smooth or rough phenotypes (Fig. 2 B, C). Until day 3, all isolates grew exponentially and entered afterwards a stationary phase. Interestingly, the CFU determination demonstrated that the isolates belonging to the same morphotype grew similarly, while different morphotypes differed by around 1 $\log_{10}$ step from day 3 on, which may be explained by stronger aggregation of rough isolates (Fig. 2 A).

3.3. Biofilm structure and composition

The architecture of the biofilms on PGBs was analyzed by scanning electron microscopy (SEM). The organization of biofilms from smooth and rough isolates differed tremendously. While the smooth isolates covered the complete surface of the glass particles almost as mono- and oligolayers (Fig. 3 A-D), the rough isolates formed huge cluster aggregates, particularly in the pores between glass particles (Fig. 3 E-G).

The rough isolate *M. abscessus* 35/14^{rg} developed aggregates of bacteria with a size of up to almost 0.5 mm that attached to the glass particles at only few spots (Fig. 3 E, G). The majority of bacteria in theses aggregates was densely aggregated (Fig. 3 F, G).

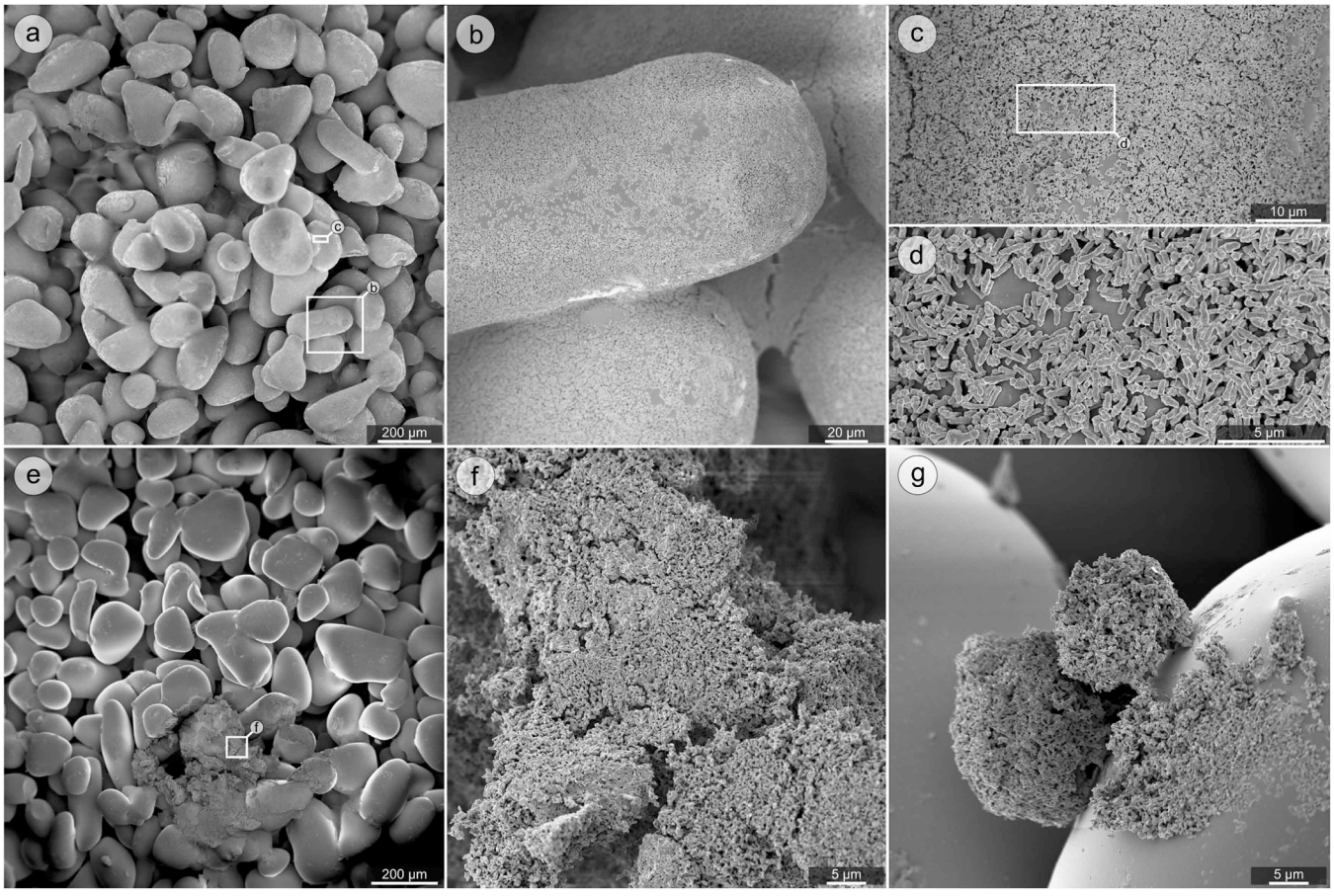

Fig. 3. Structure of *M. abscessus* 25/14^{sm} (A-D) & 35/14^{rg} (E-G) biofilms visualized by Scanning Electron Microscopy (SEM). Biofilms were grown on porous glass beads in MB-OADC for 7 days. *M. abscessus* 25/14^{sm} formed biofilm in a mono- to oligolayered structure evenly covering the surface of the glass beads (A-D). In contrast, *M. abscessus* 35/14^{rg} grew as one major aggregate with densely packed bacteria (E-G). The aggregates were partially attached to the glass surface (G), though the most of the bacteria aggregated to each other. MB-OADC: Middlebrook 7H9 broth + 10% OADC.

By quantifying molecular components of biofilm and suspension samples, we found that all four isolates produced more biomass composed of DNA, proteins and lipids per bacterium when cultivated as biofilm (Fig. 4). For the isolates *M. abscessus* 25/14^{sm} and 58/15^{rg}, a statistically significant difference ($p < 0.05$) in biomass between both cultivation forms was determined, while in the other two isolates the difference did not reach statistical significance.

Most interestingly, all four isolates produced additional DNA when they were grown as biofilms. While in suspension as planktonic bacteria, the amount of DNA per bacterium ranged around 1 pg, in the biofilms of all isolates an amount of around 15 to 30 pg of DNA per bacterium could be detected (Fig. 4; green bars).

The amount of detectable proteins per bacterium was enhanced in the biofilm-associated bacteria of 25/14^{sm}, 35/14^{rg} and 58/15^{rg}, while in 09/13^{sm} the suspension contained slightly more proteins when compared to the biofilm (Fig. 4; blue bars).

All isolates produced relatively similar amounts of lipids per bacterium that did not differ significantly between biofilm and suspension with the exception of 58/15^{rg}. In biofilm, this isolate produced more lipids compared to the others, while in suspension it displayed less lipids (Fig. 4; red bars).

3.4. Antibiotic susceptibility of M. abscessus in biofilm and suspension

Antibiotic susceptibility was tested for amikacin (AMI), which in higher concentrations shows bactericidal activity against NTM, and tigecycline (TGC), which has a bacteriostatic effect on NTM. According to CLSI guidelines, *M. abscessus* is considered to be susceptible to AMI if MIC < = 16, while no breakpoints are provided for TGC (Woods and Conville, 2011). Antibiotic susceptibility testing revealed that the biofilms of all four isolates provided higher resistance compared to the suspension cultures to both antibiotics (Fig. 5).

Especially against AMI, the biofilm showed no reduction of viable bacteria (with exception of slight reduction at 128 µg/ml in 35/14^{rg}), whereas in suspension three of the four isolates (25/14^{sm}, 35/14^{rg}, 09/13^{sm}) displayed a strong reduction at the breakpoint of 16 µg/ml, and isolate 58/15^{rg} was strongly reduced at 32 µg/ml AMI (Fig. 5 A).

Also, for TGC, it could be observed that the biofilms were not or only slightly affected by the antibiotic (Fig. 5 B). At the highest TGC concentration of 8 µg/ml, the CFU in suspension was reduced by at least

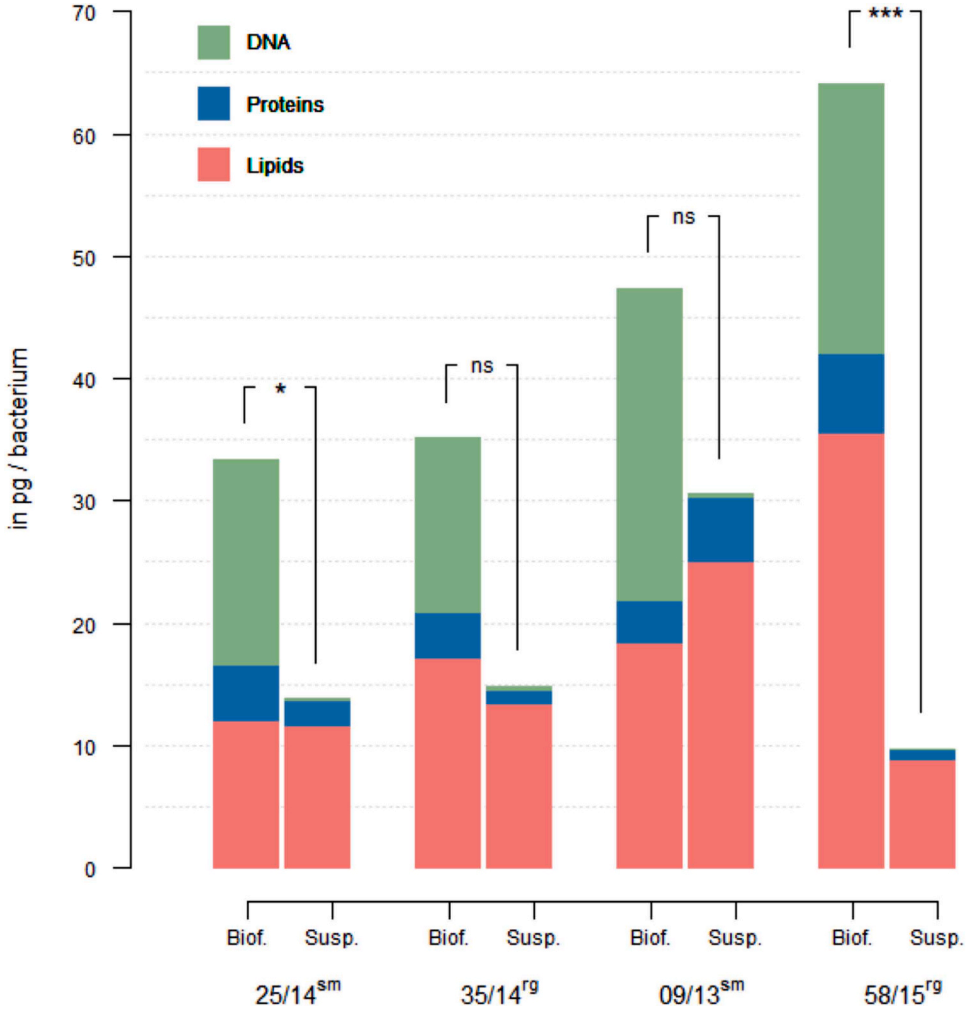

Fig. 4. Amount of proteins, lipids and DNA biomass in biofilm and suspension. Displayed are the amounts of the biofilm ECM components protein (blue), lipid (red) and DNA (green) in pg per bacterium from biofilm (24 beads with *M. abscessus* biofilm grown for 7 days in MB-OADC) and suspension (5 well grown agar plates) grown for 7 days of smooth and rough *M. abscessus* isolates. For all isolates, the amount of total biomass was higher in the biofilm samples than in the corresponding suspension. Only for *M. abscessus* 09/13^{sm} the amount of lipids and proteins was slightly higher in suspension when compared to the biofilm. The highest amount of biomass was found in *M. abscessus* 58/15^{rg}, which was a strongly significant difference to the suspension. In biofilm, this isolate produced 3.5-fold more lipids than in suspension. In all isolates, the amount of DNA in pg/bacterium was much higher in the biofilm (15 – 30 pg/bacterium) than in the suspension (0.5 – 1.5 pg/bacterium). Significance testing was performed using Wilcoxon-Rank-Sum test and significance levels were defined as follows: ns = not significant $p \geq 0.05$; * = $p \leq 0.05$; ** = $p \leq 0.01$ and *** = $p \leq 0.001$. ECM: Extracellular Matrix; MABS: *M. abscessus;* MB-OADC: Middlebrook 7H9 broth + 10% OADC.

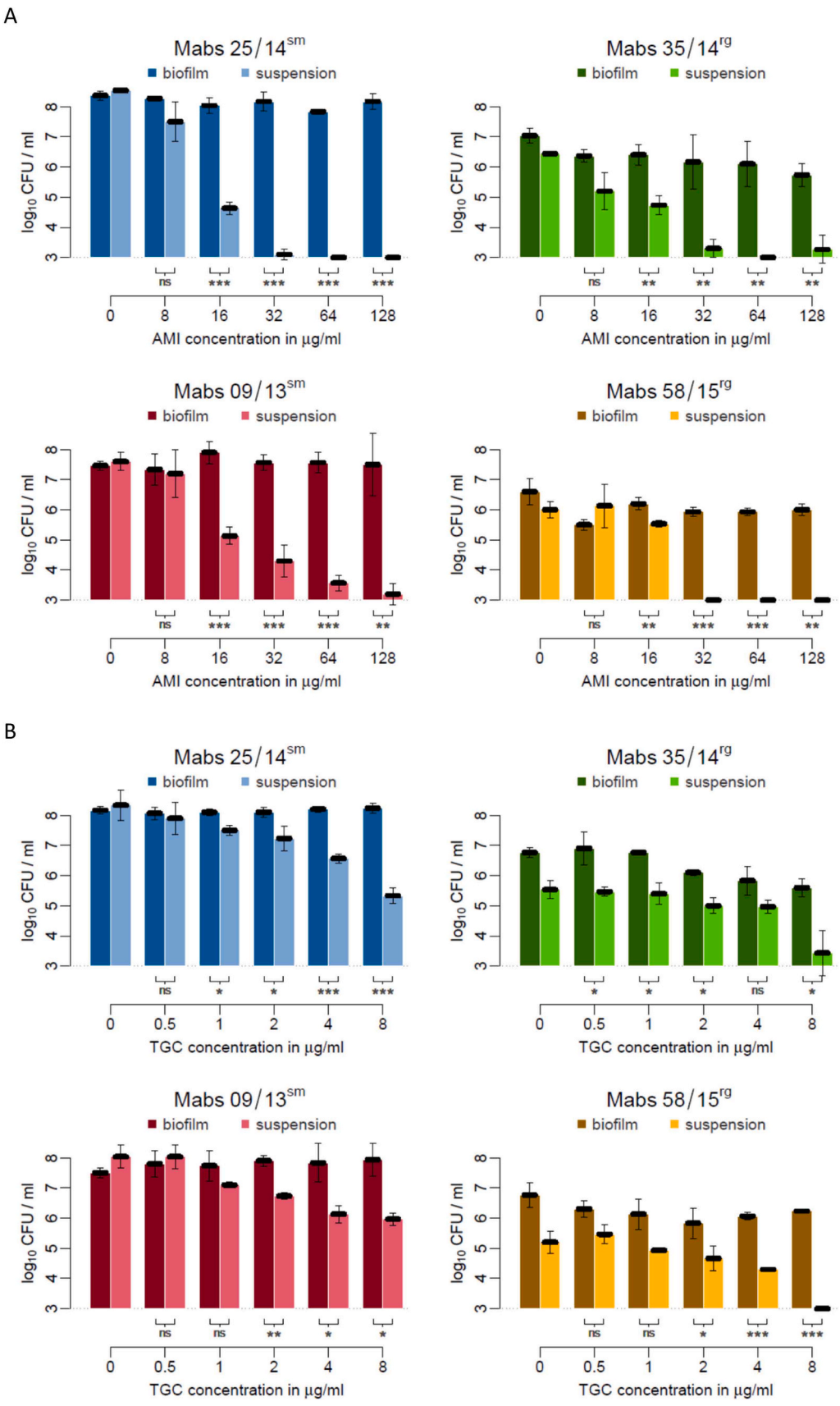

(caption on next page)

Fig. 5. Susceptibility of *M. abscessus* biofilm and suspension to amikacin and tigecycline. Biofilms and suspensions of *M. abscessus* grown for 7 days in MB-OADC were treated for 5 days with different concentrations of amikacin and tigecycline, respectively. Then, the bacteria were quantified by CFU counting. For both antibiotics, the biofilms showed increased resistance when compared to the corresponding suspension. Displayed are means and standard deviation of three individual experiments (each in triplicates). Significance testing was performed using Wilcoxon-Rank-Sum test and significance levels were defined as follows: ns = not significant $p \geq 0.05$; * = $p \leq 0.05$; ** = $p \leq 0.01$ and *** = $p \leq 0.001$. AMI: amikacin, TGC: tigecycline, MABS: *M. abscessus*.

2 $\log_{10}$ compared to the control without antibiotics. In contrast, the CFU in the biofilms of the smooth isolates stayed constant over all TCG concentrations and the number of CFU in the biofilms of rough isolates decreased by max. 0.9 $\log_{10}$ only.

3.5. Disinfectant tolerance of *M. abscessus* in biofilm and suspension

Disinfectant tolerance was tested for two agents of different mode of action: glutaraldehyde, which is a fixative agent cross-linking cell envelope proteins (McDonnell and Russell, 1999) and peracetic acid, which works as oxidative agent.

The effectivity testing with GA showed that biofilm formation provided an enhanced tolerance to GA compared to suspension for smooth isolates *M. abscessus* isolate 09/13^{sm} and 25/14^{sm} when disinfected with concentrations at or above 0.5% GA (v/v) (Fig. 6 A). For the rough isolates 35/14^{rg} and 58/15^{rg}, a statistically significant increased tolerance of the biofilm compared to suspension could only be observed for isolate 58/15^{rg} at 5% GA (Fig. 6 A).

When disinfected with PAA, the biofilms of all isolates showed enhanced tolerance when compared to the suspension (Fig. 6 B). The suspensions of isolates 25/14^{sm}, 09/13^{sm} and 58/15^{rg} were reduced to the detection limit (3 $\log_{10}$ CFU/ml) at 0.05% PAA (v/v), and isolate 35/14^{rg} reached the detection limit at 0.075% (v/v). In contrast, the biofilms were first reduced completely between 0.1% and 0.5% PAA (v/v). Biofilm from isolate 09/13^{sm} showed the highest tolerance against PAA with considerable growth at even 0,1% PAA (Fig. 6 B).

4. Discussion

The formation of biofilm can contribute to an increase in resistance toward antimicrobial substances (Flemming et al., 2016). In species like *M. abscessus* that already display a high innate resistance to most antimicrobials, the development of a biofilm can worsen the problem. As biofilms of *M. abscessus* have already been documented in patients (Qvist et al., 2015), research on mycobacterial biofilms is essential to improve treatment options and of prevention measures (Chakraborty and Kumar, 2019; Esteban and García-Coca, 2017).

The model system chosen for generation and cultivation of biofilms has significant impact on the outcome of the experiments (Azeredo et al., 2017). The structural properties of the porous glass beads enabled surface-attached biofilm formation for both, smooth and rough *M. abscessus* isolates. To our knowledge, surface-attached biofilms of rough *M. abscessus* isolates were not yet documented by others. Our cultivation technique using PGB enabled visualization of formation of surface-attached biofilms of rough *M. abscessus* variants. This is surely influenced by the properties of the porous glass beads, which provide fine-graded shear forces from zero at the bottom of the 60 μm pores to high at the PGB's outer surface, depending on the degree of agitation. Moreover, other experimental conditions (e.g. medium, pH, temperature, etc.) also influence biofilm formation tremendously (Flemming et al., 2016) (Azeredo et al., 2017). In order to stay close to the official protocols for disinfectant testing and antibiotic testing, we cultivated the bacteria in standard mycobacteria media, which contain Tween 80. Tween 80 alters the ability of mycobacteria to aggregate and this has an impact on biofilm formation. Therefore, other cultivation media without Tween, such as for example artificial sputum media, should be examined for their suitability in antimicrobial resistance testing systems. While the PGB system is a relevant model to mimic surfaces such as those present in water distribution systems or medical instruments, alternative models will have to be established as surrogate for tissue.

The aggregation of rough *M. abscessus* variants is a common problem when working with these morphotypes that also influenced the CFU counting in our experiments. Because of the strong cell-cell adhesion it is almost impossible to individualize the bacteria completely and ensure a correct CFU counting. The number of bacteria in our biofilm growth curves displayed a one $\log_{10}$-fold difference in CFU count between smooth and rough isolates.

A convincing alternative to CFU counting for quantifying *M. abscessus* is qPCR with prior addition of PMA to the sample, which ensures that only DNA of viable bacteria is amplified. Using this method for growth curve analysis almost no differences in measured genome equivalents of all four isolates could be detected. This provides evidence, that the total number of bacteria was equal between smooth and rough isolates in biofilms. As PMA-qPCR was shown to be inappropriate for quantification of mycobacteria after disinfection by e.g. chlorine (Lee et al., 2015), we decided to use CFU counting to conclude on the effects of antimicrobials in specific isolates and growth conditions.

Although both morphotypes showed similar biofilm biomass, the organization of the biofilms differed enormously. While smooth isolates covered the complete glass surface in an almost monolayered film, the rough variants preferred cell-cell adhesion and showed reduced surface attachment. It is known, that besides other properties, the hydrophobicity of the surface or the bacteria themselves plays an important role in surface adhesion. The lack of GPL causes an enhanced hydrophobicity of rough *M. abscessus* variants (Viljoen et al., 2018) and triggers bacterial interaction (Llorens-Fons et al., 2017). Nessar et al. (Nessar et al., 2011), demonstrated that the deletion of the *mmpL4b* gene, which also contributes to the GPL presence on the cell surface, results in a decreased capability of surface attachment by *M. abscessus*. Our results support the hypothesis that the architectural differences in biofilm appearance and the capability of the bacteria to attach to a surface are mainly determined by the presence of GPL in *M. abscessus*.

The biofilm matrix consists of multiple different substances (Richards and Ojha, 2014). Here, we analyzed DNA, lipids and proteins with respect to their overall amount in the biofilm. Due to the higher complexity that the analysis of polysaccharides holds, we did not yet include these in our experimental set up. Other research has provided more detailed information about which substances contribute to the biofilm matrix of NTM (Chakraborty and Kumar, 2019).

The general molecular composition of the biofilm (relative amounts of DNA, proteins, lipids) did not differ much between all four isolates. Most interestingly, the amount of DNA was significantly higher ($P < 0.05$; data not separately shown) in all biofilm samples compared to the corresponding suspensions, which might be due to the production of extracellular DNA. We conclude that the presence of eDNA is an important factor for the biofilm composition of *M. abscessus* regardless of the morphotype. eDNA is known to contribute considerably to the structural integrity of the biofilm, often forming net-like structures (Saxena et al., 2019). The role of eDNA in *M. avium* biofilms was extensively analyzed by (Rose et al., 2015). The authors showed that by DNase treatment, the formation of biofilm could be prevented and disturbed and, moreover that the susceptibility of the bacteria against antibiotics was increased. Due to the innate resistance of NTM to many antimicrobial substances, the usage of DNase was meanwhile discussed as a potential option to improve treatment success (Aung et al., 2016; Chakraborty and Kumar, 2019). In patients with CF the use of inhaled recombinant human DNAse has been tested by various groups and seems to stabilize the lung function as well as increase the expectoration of

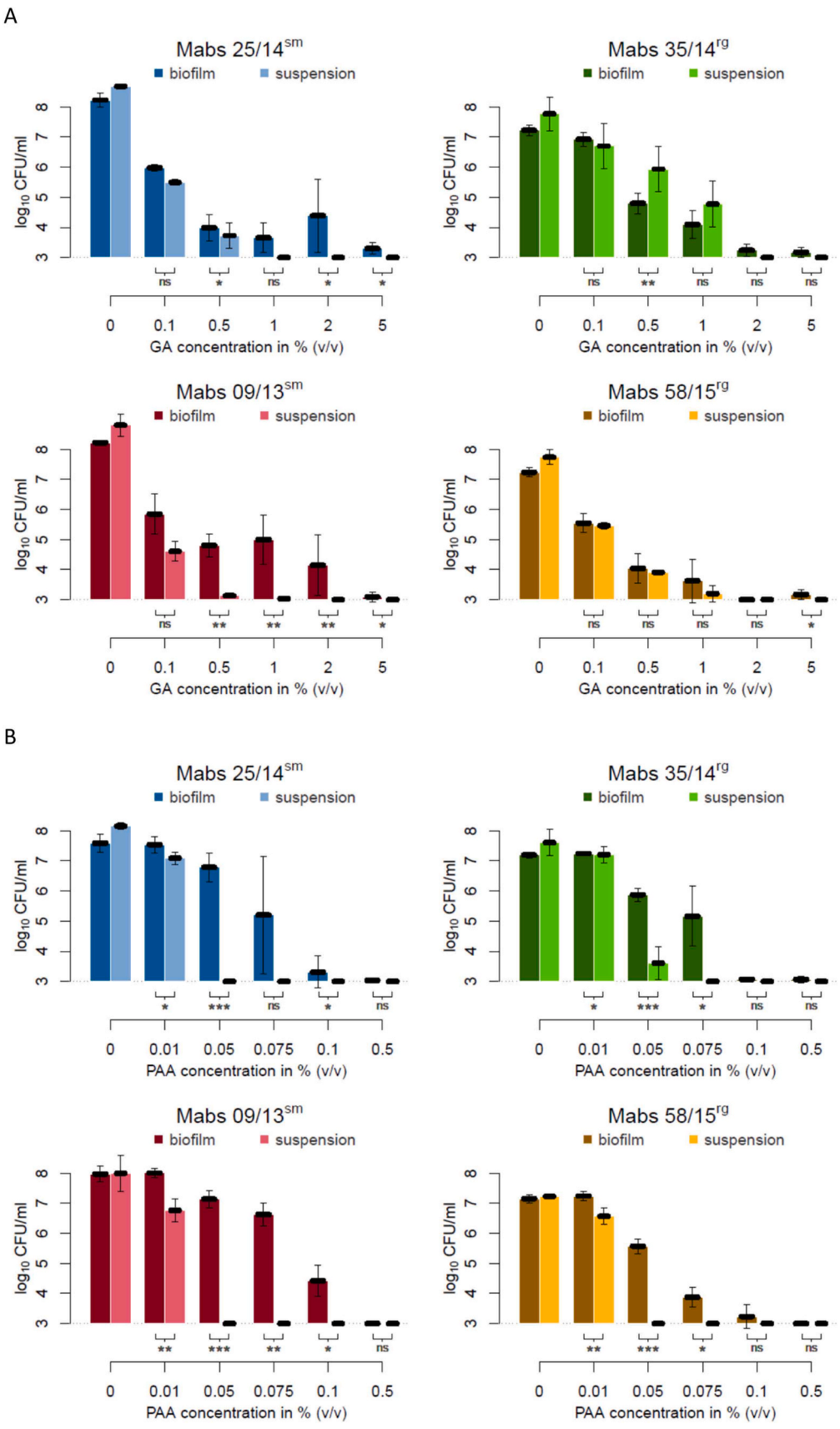

(caption on next page)

Fig. 6. Tolerance of *M. abscessus* biofilm and suspension towards glutaraldehyde and peracetic acid. Biofilms and suspensions of *M. abscessus* grown for 7 days in MB-OADC were exposed to increasing concentrations of GA and PAA. Especially at higher concentrations the tolerance of the biofilm was higher than for the corresponding suspension. Displayed are means and standard deviations of three individual biological replicates (each in triplicates). Significance testing was performed using Wilcoxon-Rank-Sum test and significance levels were defined as follows: ns = not significant $p \geq 0.05$; * = $p \leq 0.05$; ** = $p \leq 0.01$ and *** = $p \leq 0.001$. GA: glutaraldehyde; PAA: peracetic acid.

thickened sputum (Shak, 1995).

Biofilms as natural mode of living of most bacteria attract increasing attention also because of their effects on disinfection procedures in medical settings and on the efficacy of antibiotic treatments of patients. We therefore selected two disinfectants and two antibiotics to explore the importance of *M. abscessus* biofilms for their administration. GA and PAA were selected as disinfectants because they are also used for disinfection of medical devices such as HCUs and because they represent two different classes of disinfectants (fixative: GA, oxidative: PAA). AMI and TGC both are important antibiotics for treatment of *M. abscessus* infections and are representatives of the classes of bacteriostatic (TGC) and bactericidal (AMI) antibiotics. Although smooth and rough morphotypes differed greatly in their overall biofilm structure, they displayed similar antimicrobial susceptibility patterns.

Biofilms from smooth and rough isolates were more tolerant to PAA than the corresponding planktonic bacteria in suspension. The biofilm of the smooth isolates also exhibited increased tolerance to GA. Overall, the biofilms from the smooth isolates showed a higher tolerance/resistance towards tested antimicrobials in relation to the suspensions than the biofilms from the rough ones. By taking into consideration that the composition of the biofilm matrix from paired rough and smooth isolates was similar, the increase in tolerance might be more likely influenced by the architecture of the biofilm than by its matrix components. We expected that the aggregative biofilm of the rough isolates, in which a large number of bacteria were protected from direct external influences, would provide better protection than the monolayered biofilm of the smooth isolates. One explanation for reduced tolerance of biofilms from rough compared to smooth isolates may be the lack of nutrients and oxidative stress that the rough bacteria face in the inner parts of the compact aggregates. We assume that the conditions in the different biofilm models affect the results of the susceptibility testing. Further investigations on differently cultivated biofilms are needed to evaluate, which method provides the most relevant results. Also, clarification is needed on the effect of biofilms of different colony morphotypes of *M. abscessus* on disease development and antibiotic resistance within the tissues of patients.

5. Conclusion

Smooth and rough *M. abscessus* variants are able to form surface-attached biofilms on PGBs. We were able to show that the proportions of DNA, proteins and lipids did not differ much between both morphotypes. An important finding is that the production of eDNA was significantly higher in the biofilm samples of all tested isolates when compared to the suspension samples. The discrepancy between resistance of biofilm-grown *M. abscessus* compared to suspension culture underlines the need to adjust current recommendations for antibiotic susceptibility testing and disinfectant testing to meet the relevant physiological growth conditions of these bacteria.

Funding

Funding was provided by the Robert Koch Institute, Berlin, Germany. This research did not receive any specific grant from funding agencies in the public, commercial, or not-for-profit sectors.

CRediT authorship contribution statement

Anna Maria Oschmann-Kadenbach: Formal analysis, Investigation, Methodology, Validation, Visualization, Writing – original draft. **Christoph Schaudinn:** Investigation, Methodology. **Leonard Borst:** Methodology. **Carsten Schwarz:** Resources. **Katharina Konrat:** Methodology, Supervision. **Mardjan Arvand:** Conceptualization, Supervision, Writing – review & editing. **Astrid Lewin:** Conceptualization, Supervision, Writing – review & editing.

Declaration of Competing rInterest

The authors declare that they have no known competing financial interests or personal relationships that could have appeared to influence the work reported in this paper.

Acknowledgements

We gratefully thank Linus Fiedler for supporting the execution of experiments and to Hubert Schäfer for help with GPL analysis. We are further grateful to Genna Sohl for language correction.

Appendix A. Supporting information

Supplementary data associated with this article can be found in the online version at doi:10.1016/j.ijmm.2024.151603.

References

Aung, T.T., Yam, J.K., Lin, S., Salleh, S.M., Givskov, M., Liu, S., Lwin, N.C., Yang, L., Beuerman, R.W., 2016. Biofilms of pathogenic nontuberculous mycobacteria targeted by new therapeutic approaches. Antimicrob. Agents Chemother. 60, 24–35.

Azeredo, J., Azevedo, N.F., Briandet, R., Cerca, N., Coenye, T., Costa, A.R., Desvaux, M., Di Bonaventura, G., Hébraud, M., Jaglic, Z., Kačániová, M., Knøchel, S., Lourenço, A., Mergulhão, F., Meyer, R.L., Nychas, G., Simões, M., Tresse, O., Sternberg, C., 2017. Critical review on biofilm methods. Crit. Rev. Microbiol. 43, 313–351.

Baker, A.W., Lewis, S.S., Alexander, B.D., Chen, L.F., Wallace, R., Brown-Elliott, B.A., Isaacs, P.J., Pickett, L.C., Patel, C.B., Smith, P.K., Reynolds, J.M., Engel, J., Wolfe, C. R., Milano, C.A., Schroder, J.N., Davis, R.D., Hartwig, M.G., Stout, J.E., Strittholt, N., Maziarz, E.K., Saullo, J.H., Hazen, K.C., Walczak, R.J., Jr, Vasireddy, R., Vasireddy, S., McKnight, C.M., Anderson, D.J., Sexton, D.J., 2017. Two-phase hospital-associated outbreak of Mycobacterium abscessus: investigation and mitigation. Clin. Infect. Dis. 64, 902–911.

Benwill, J.L., Wallace, R.J., 2014. Mycobacterium abscessus: challenges in diagnosis and treatment. Curr. Opin. Infect. Dis. 27, 506–510.

Bernut, A., Herrmann, J.L., Kissa, K., Dubremetz, J.F., Gaillard, J.L., Lutfalla, G., Kremer, L., 2014. Mycobacterium abscessus cording prevents phagocytosis and promotes abscess formation. Proc. Natl. Acad. Sci. 111, E943–E952.

Chakraborty, P., Kumar, A., 2019. The extracellular matrix of mycobacterial biofilms: could we shorten the treatment of mycobacterial infections? Microbe Cell 6, 105–122.

Clary, G., Sasindran, S.J., Nesbitt, N., Mason, L., Cole, S., Azad, A., McCoy, K., Schlesinger, L.S., Hall-Stoodley, L., 2018. Mycobacterium abscessus smooth and rough Morphotypes form antimicrobial-Tolerant biofilm phenotypes but are killed by acetic acid. Antimicrob. Agents Chemother. 62.

Esteban, J., García-Coca, M., 2017. Mycobacterium biofilms. Front. Microbiol. 8, 2651.

Falkinham, J.O.Disinfection and cleaning of heater-cooler units: suspension- and biofilm-killing. J. Hosp. Infect., 3rd Ed., 2020.

Flemming, H.C., Wingender, J., Szewzyk, U., Steinberg, P., Rice, S.A., Kjelleberg, S., 2016. Biofilms: an emergent form of bacterial life. Nat. Rev. Microbiol. 14, 563–575.

Howard, S.T., Rhoades, E., Recht, J., Pang, X., Alsup, A., Kolter, R., Lyons, C.R., Byrd, T. F., 2006. Spontaneous reversion of Mycobacterium abscessus from a smooth to a rough morphotype is associated with reduced expression of glycopeptidolipid and reacquisition of an invasive phenotype. Microbiology 152, 1581–1590.

Kim, B.R., Kim, B.J., Kook, Y.H., Kim, B.J., 2019. Phagosome escape of rough Mycobacterium abscessus strains in murine macrophage via phagosomal rupture can lead to type i interferon production and their cell-to-cell spread. Front. Immunol. 10, 125.

Kirubakar, G., Schäfer, H., Rickerts, V., Schwarz, C., Lewin, A., 2020. Mutation on lysX from Mycobacterium avium hominissuis impacts the host-pathogen interaction and virulence phenotype. Virulence 11, 132–144.

Konrat, K., Schwebke, I., Laue, M., Dittmann, C., Levin, K., Andrich, R., Arvand, M., Schaudinn, C., 2016. The bead assay for biofilms: a quick, easy and robust method for testing disinfectants. PLOS One 11, e0157663.
Kreutzfeldt, K.M., McAdam, P.R., Claxton, P., Holmes, A., Seagar, A.L., Laurenson, I.F., Fitzgerald, J.R., 2013. Molecular longitudinal tracking of mycobacterium abscessus spp. during chronic infection of the human lung. PLOS ONE 8.
Lee, E.S., Lee, M.H., Kim, B.S., 2015. Evaluation of propidium monoazide-quantitative PCR to detect viable Mycobacterium fortuitum after chlorine, ozone, and ultraviolet disinfection. Int. J. Food Microbiol. 210, 143–148.
Lewin, A., Freytag, B., Meister, B., Sharbati-Tehrani, S., Schäfer, H., Appel, B., 2003. Use of a quantitative TaqMan-PCR for the fast quantification of mycobacteria in broth culture, eukaryotic cell culture and tissue. J. Vet. Med. Ser. B: Infect. Dis. Vet. Public Health 50, 505–509.
Lewin, A., Kamal, E., Semmler, T., Winter, K., Kaiser, S., Schäfer, H., Mao, L., Eschenhagen, P., Grehn, C., Bender, J., Schwarz, C., 2021. Genetic diversification of persistent Mycobacterium abscessus within cystic fibrosis patients. Virulence 12, 2415–2429.
Llorens-Fons, M., Pérez-Trujillo, M., Julián, E., Brambilla, C., Alcaide, F., Byrd, T.F., Luquin, M., 2017. Trehalose polyphleates, external cell wall lipids in Mycobacterium abscessus, are associated with the formation of clumps with cording morphology, which have been associated with virulence. Front. Microbiol. 8, 1402.
López-Roa, P., Esteban, J., Muñoz-Egea, M.C., 2022. Updated review on the mechanisms of pathogenicity in Mycobacterium abscessus, a rapidly growing emerging pathogen. Microorganisms 11.
McDonnell, G., Russell, A.D., 1999. Antiseptics and disinfectants: activity, action, and resistance. Clin. Microbiol. Rev. 12, 147–179.
Nessar, R., Reyrat, J.M., Davidson, L.B., Byrd, T.F., 2011. Deletion of the mmpL4b gene in the Mycobacterium abscessus glycopeptidolipid biosynthetic pathway results in loss of surface colonization capability, but enhanced ability to replicate in human macrophages and stimulate their innate immune response. Microbiology 157, 1187–1195.
Pawlik, A., Garnier, G., Orgeur, M., Tong, P., Lohan, A., Le Chevalier, F., Sapriel, G., Roux, A.L., Conlon, K., Honore, N., Dillies, M.A., Ma, L., Bouchier, C., Coppee, J.Y., Gaillard, J.L., Gordon, S.V., Loftus, B., Brosch, R., Herrmann, J.L., 2013. Identification and characterization of the genetic changes responsible for the characteristic smooth-to-rough morphotype alterations of clinically persistent Mycobacterium abscessus. Mol. Microbiol. 90, 612–629.
Petrini, B., 2006. Mycobacterium abscessus: an emerging rapid-growing potential pathogen. APMIS 114, 319–328.
Phillips, M.S., von Reyn, C.F., 2001. Nosocomial infections due to nontuberculous mycobacteria. Clin. Infect. Dis. 33, 1363–1374.
Primm, T.P., Lucero, C.A., Falkinham Iii, J.O., 2004. Health impacts of environmental Mycobacteria. Clin. Microbiol. Rev. 17, 98–106.
Qvist, T., Eickhardt, S., Kragh, K.N., Andersen, C.B., Iversen, M., Hoiby, N., Bjarnsholt, T., 2015. Chronic pulmonary disease with Mycobacterium abscessus complex is a biofilm infection. Eur. Respir. J. 46, 1823–1826.
Riccardi, N., Monticelli, J., Antonello, R.M., Luzzati, R., Gabrielli, M., Ferrarese, M., Codecasa, L., Di Bella, S., Giacobbe, D.R., 2020. Mycobacterium chimaera infections: an update. J. Infect. Chemother. 26, 199–205.
Richards, J.P., Ojha, A.K., 2014. Mycobacterial biofilms. Microbiol. Spectr. 2.
Rose, S.J., Babrak, L.M., Bermudez, L.E., 2015. Mycobacterium avium possesses extracellular DNA that Contributes to Biofilm Formation, Structural Integrity, and Tolerance to Antibiotics. PLOS One 10, e0128772.
Ruangkiattikul, N., Rys, D., Abdissa, K., Rohde, M., Semmler, T., Tegtmeyer, P.K., Kalinke, U., Schwarz, C., Lewin, A., Goethe, R., 2019. Type I interferon induced by TLR2-TLR4-MyD88-TRIF-IRF3 controls Mycobacterium abscessus subsp. abscessus persistence in murine macrophages via nitric oxide. Int. J. Med. Microbiol. 309, 307–318.
Saxena, P., Joshi, Y., Rawat, K., Bisht, R., 2019. Biofilms: architecture, resistance, quorum sensing and control mechanisms. Indian J. Microbiol. 59, 3–12.
Schreiber, P.W., Kuster, S.P., Hasse, B., Bayard, C., Rüegg, C., Kohler, P., Keller, P.M., Bloemberg, G.V., Maisano, F., Bettex, D., Halbe, M., Sommerstein, R., Sax, H., 2016. Reemergence of Mycobacterium chimaera in heater-cooler units despite intensified cleaning and disinfection protocol. Emerg. Infect. Dis. 22, 1830–1833.
Shak, S., 1995. Aerosolized recombinant human DNase I for the treatment of cystic fibrosis. Chest 107, 65s–70s.
Steindor, M., Nkwouano, V., Mayatepek, E., Mackenzie, C.R., Schramm, D., Jacobsen, M., 2015. Rapid detection and immune characterization of Mycobacterium abscessus infection in cystic fibrosis patients. PLOS One 10, e0119737.
van Ingen, J., Kuijper, E.J., 2014. Drug susceptibility testing of nontuberculous mycobacteria. Future Microbiol. 9, 1095–1110.
Viljoen, A., Gutierrez, A.V., Dupont, C., Ghigo, E., Kremer, L., 2018. A simple and rapid gene disruption strategy in Mycobacterium abscessus: on the design and application of glycopeptidolipid mutants. Front. Cell Infect. Microbiol. 8, 69.
Woods G.L., B.E.B., Conville P.S. ,et al., Susceptibility Testing of Mycobacteria, Nocardiae, and Other Aerobic Actinomycetes. Clinical and Laboratory Standards Institute 2nd edition, 2011.
Zoppo, M., Di Luca, M., Franco, M., Rizzato, C., Lupetti, A., Stringaro, A., De Bernardis, F., Schaudinn, C., Barrasa, M.I., Bottai, D., Vyas, V.K., Tavanti, A., 2020. CpALS4770 and CpALS4780 contribution to the virulence of Candida parapsilosis. Microbiol. Res. 231, 126351.